Research paper

Dissolution behavior of co-amorphous amino acid-indomethacin mixtures: The ability of amino acids to stabilize the supersaturated state of indomethacin

Rami Ojarinta, Aki T. Heikkinen, Elina Sievänen, Riikka Laitinen

PII: S0939-6411(16)30584-7
DOI: http://dx.doi.org/10.1016/j.ejpb.2016.11.023
Reference: EJPB 12358

To appear in: *European Journal of Pharmaceutics and Biopharmaceutics*

Received Date: 22 September 2016
Revised Date: 16 November 2016
Accepted Date: 17 November 2016

Please cite this article as: R. Ojarinta, A.T. Heikkinen, E. Sievänen, R. Laitinen, Dissolution behavior of co-amorphous amino acid-indomethacin mixtures: The ability of amino acids to stabilize the supersaturated state of indomethacin, *European Journal of Pharmaceutics and Biopharmaceutics* (2016), doi: http://dx.doi.org/10.1016/j.ejpb.2016.11.023

Dissolution behavior of co-amorphous amino acid-indomethacin mixtures: The ability of amino acids to stabilize the supersaturated state of indomethacin

Rami Ojarinta[a,*], Aki T. Heikkinen[b,a], Elina Sievänen[c], Riikka Laitinen[a]

[a] School of Pharmacy, University of Eastern Finland, P.O. Box 1627, 70211 Kuopio, Finland

[b] Admescope Ltd, Typpitie 1, 90620 Oulu, Finland

[c] Department of Chemistry, University of Jyväskylä, P.O. Box 35, 40014 University of Jyväskylä, Finland

*Corresponding author:

Tel. +358 40 355 3870

E-mail: rami.ojarinta@uef.fi

ABSTRACT

Arginine, phenylalanine, and tryptophan have been previously shown to improve the solid-state stability of amorphous indomethacin. The present study investigates the ability of these amino acids to prolong the supersaturation of indomethacin in both aqueous and biorelevant conditions either when freely in solution or when formulated as co-amorphous mixtures.

The co-amorphous amino acid-indomethacin mixtures (molar ratio 1:1) and amorphous indomethacin were prepared by cryomilling. Dissolution and precipitation tests were performed in buffer solutions (pH 5 and 6.5) and in Fed and Fasted State Simulated Intestinal Fluids (FeSSIF and FaSSIF, respectively). Precipitation tests were conducted with the solvent shift method. The supersaturation stability of indomethacin and the precipitation inhibitory effect of amino acids were evaluated by calculating the supersaturation factor and the excipient gain factor, respectively.

Biorelevant media exerted a significant effect on indomethacin solubility but had little effect on the supersaturation stability. Arginine had the most significant impact on the dissolution properties of indomethacin, but also phenylalanine and tryptophan stabilized supersaturation in some media when formulated as co-amorphous mixtures with indomethacin. Only arginine stabilized supersaturation without co-amorphization, an effect only observed in media of pH 6.5. The unique behavior of the arginine-indomethacin mixture was further demonstrated by the abrupt formation of a precipitate, when an excess physical mixture of arginine and indomethacin was added to FeSSIF (pH 6.5). The solid-state investigation of this precipitate indicated that it probably consisted of crystalline arginine-indomethacin salt with possibly some residual crystalline starting materials.

KEYWORDS: Co-amorphous, amino acid, supersaturation, precipitation, biorelevant

ABBREVIATIONS

AA: amino acid

ACN: acetonitrile

ARG: arginine

AUC: area under the curve

CA: co-amorphous

DMSO: dimethyl sulfoxide

DS: degree of supersaturation

DSC: differential scanning calorimetry

EGF: excipient gain factor

FaSSIF: fasted state simulated intestinal fluid

FeSSIF: fed state simulated intestinal fluid

FTIR: Fourier transform infrared spectroscopy

HPLC: high performance liquid chromatography

IND: indomethacin

PHE: phenylalanine

PM: physical mixture

SF: supersaturation factor

ssNMR: solid-state nuclear magnetic resonance spectroscopy

TFA: trifluoro acetic acid

$T_{g:}$ glass transition temperature

T_m: melting temperature

TRP: tryptophan

XRPD: X-ray powder Diffractometry.

1. INTRODUCTION

Orally administered drugs must have sufficient water solubility to ensure their bioavailability and pharmacological activity [1]. However, modern drug development often is seeking to achieve higher pharmacological potency by increasing the drug's molecular weight and lipophilicity [2,3]. In these cases, the limited water solubility may become a major challenge for successful formulation. Takagi et al. investigated the solubilities of the 200 most popular drugs in four developed countries; approximately 40% of these drugs were considered as being practically insoluble [4]. In particular, the impact of higher lipophilicity was noteworthy among newly discovered and developed drugs.

Aqueous solubility may not provide a sufficiently comprehensive perspective of the dissolution behavior of a drug in the gastrointestinal tract since there are numerous factors, such as differences in pH and the presence of naturally occurring surfactants and food components, which may influence the dissolution process [5]. To overcome this challenge, fluids that simulate gastric or intestinal fluids, and are easy to prepare in the laboratory, have been introduced [5,6]. These include for example fasted state simulated intestinal fluid (FaSSIF) and fed state simulated intestinal fluid (FeSSIF) which have been found to predict drug solubility in actual human intestinal fluid with sufficient accuracy in the early stages of drug development [6].

If a drug is highly permeable but poorly soluble (Biopharmaceutical Classification System class II), dissolution may limit the rate of absorption; hence manipulating solubility or dissolution properties may significantly improve its bioavailability [7,8]. Converting a crystalline material into an amorphous form is one of the most promising ways to improve apparent solubility, since the maximum concentrations in solution achieved with the amorphous form may be significantly higher due to its higher internal energy than with its crystalline counterpart [9-12]. Furthermore, the increased apparent solubility does not decrease the drug's permeability through intestinal wall [13-15]. Unfortunately, the greater internal energy and molecular movement of the amorphous form may also cause the material to convert spontaneously back to its crystalline form during processing, storage or dissolution.

Amorphous solid dispersions with polymers have been extensively studied and shown to stabilize both the drug supersaturation in solution and the amorphous form in the solid state [16,17]. In a solution, an amorphous form of a drug can be described as a spring that triggers the high initial concentration whereas the polymer acts as a parachute to prevent the recrystallization and precipitation of the drug [18]. However, the use of polymers as stabilizers of the amorphous drugs has some limitations, such as the hygroscopicity of many polymers, and the limited miscibility of drugs to polymers, which results to large polymer consumption [19]. To overcome these formulation challenges, co-amorphous formulations have been introduced and shown to stabilize the amorphous form in the solid state [12, 19]. By the definition of Dengale et al., these systems contain two or more small molecular weight compounds that are homogenously mixed to form an amorphous single phase system [19]. For example, two active compounds have been combined to produce co-amorphous mixtures [20,21], but finding compatible drug-drug pairs may, however, be challenging, which has increased the interest in combining a pharmacologically active molecule with an inactive low molecular weight excipient, such as an amino acid (AA) [22-24].

Löbmann et al. studied the ability of carbamazepine and indomethacin (IND) to form co-amorphous mixtures with arginine (ARG), tyrosine, phenylalanine (PHE) and tryptophan (TRP) [24]. They noted that both drugs formed co-amorphous blends with suitable amino acids. In addition, their study demonstrated that co-amorphous blends were more stable and had higher intrinsic dissolution rates than the amorphous drugs alone. The improved solid-state stability was explained by the increased glass transition temperature (T_g) of co-amorphous blends, by the presence of stabilizing intermolecular interactions, and by the AAs acting as “impurities” at the molecular level. The improvement in the intrinsic dissolution rate was especially significant with respect to the ARG-IND co-amorphous mixtures; this was attributable to salt formation. The increased solid-state stability or intrinsic dissolution rate, however, provided no information on the ability of AAs to stabilize drug

supersaturation in solution. Therefore, producing dissolution profiles that provide information on how significant and how long-lasting supersaturation may be achieved with a particular AA-drug combination, would be very useful when evaluating the actual dissolution properties of co-amorphous formulations.

The present study examined in detail the dissolution properties of ARG-IND, PHE-IND and TRP-IND co-amorphous mixtures, which were prepared using similar methods as described by Löbmann et al. [24,25]. The aim was to investigate whether the AAs would be able to act as molecular parachutes and prolong the supersaturated state of amorphous IND in simple buffer solutions (pH 5.0 and 6.5) as well as in biorelevant solutions (FaSSIF (pH 6.5) and FeSSIF (pH 5.0), which have rarely been applied in dissolution studies with (co-)amorphous formulations [26]. Precipitation tests were conducted by the solvent shift method in buffers and biorelevant media to gather relevant information on the ability of the amino acids to maintain supersaturation when they are present freely in solution.

Interestingly, in preliminary studies (where also FaSSIF of pH 5.0 and FeSSIF of pH 6.5 were used) a precipitate was formed when the physical mixture of ARG and IND was dissolved in FeSSIF of pH 6.5. Although these media were otherwise not investigated in this study, since the effect of pH could be demonstrated with buffer solutions and these media did not resemble any physiological state, the characterization of the precipitate is included in this report.

2. MATERIALS AND METHODS

2.1 Materials

IND (γ-form) was purchased from Hangzhou Dayanchem (Hangzhou, China). ARG, PHE, and TRP were all supplied by Sigma-Aldrich Co. (St. Louis, USA).

Solvents used were acetonitrile (ACN, VWR Chemicals, Fontenay-sous-Bois, France), ultra-purified water (Elga Purelab Ultra, Model ULXXXANM2, Snr: ULT00002345), methanol (Mallinckrodt Baker B.V., Netherlands), and dimethyl sulfoxide (DMSO, Fisher Chemical, Loughborough, UK). Trifluoro acetic acid (TFA) was purchased from Alfa Aesar GmbH & co (Germany).

FeSSIF and FaSSIF were prepared by adding a commercially available SIF powder® (SIF Powder Original®, biorelevant.com, Surrey, UK) to a blank buffer (FeSSIF blank, an acetate buffer with a pH of 5.0, or FaSSIF blank, a phosphate buffer with a pH of 6.5) according to the recommendations of the SIF-powder® manufacturer (SIF Powder Original® How To Use 1.4, 2013). Sodium hydroxide (NaOH) was obtained from both Oy FF-Chemicals AB (Finland) and Mallinckrodt Baker B.V. (Netherlands), sodium dihydrogen phosphate monohydrate ($NaH_2PO_4*H_2O$) from Merck (Germany), sodium chloride (NaCl) from Mallinckrodt Baker B.V. (Netherlands) and glacial acetic acid (CH3COOH) from both VWR (France) and Riedel de Haën (Germany). The pHs of the buffer solutions were adjusted with 1 M or 5 M hydrochloric acid (HCl) or NaOH solutions (pH meter: Metrohm 744, Herisau, Switzerland; electrode: Metrohm Ag 9191 Herisau, Switzerland).

2.2 Preparation of materials for dissolution tests.

Physical mixtures of AAs and IND (AA-IND PM) were mixed by hand in a mortar. The components were mixed in a molar ratio of 1:1, which corresponds to a mass ratio of 0.49:1 for ARG-IND; 0.46:1 for PHE-IND; and 0.57:1 for TRP-IND.

Co-amorphous AA-IND (AA-IND CA) mixtures were prepared by cryomilling (MM400, Retsch GmbH, Haan, Germany). In addition, pure IND was milled to produce amorphous IND. Subsequently, 500 mg of AA-IND PM or pure IND were milled in 25 ml milling chambers containing two 12 mm stainless steel balls at 30 Hz for 60 min. The milling chambers were placed every 10 min in liquid nitrogen for 2 minutes to prevent unwanted solid-state transformations or degradation caused by heat.

AA-IND CAs and amorphous IND were stored in refrigerator (approximately 5 °C) at 0 % relative humidity (RH) (phosphorus pentoxide).

2.3 Dissolution tests

The dissolution tests were performed in triplicate in 50 ml Erlenmeyer flasks that were held in a shaking water bath (Grant OLS 200, sr. nr. 8Q0037005, England). The temperature of the water bath was 37 °C and the shaking speed was set at 130 rpm. FaSSIF blank (pH 6.5), FeSSIF blank (pH 5.0), FaSSIF (pH 6.5) and FeSSIF (pH 5.0) were used as dissolution media. Since precipitation tests were intended to be performed by the solvent shift method, 2 % of DMSO was added to the dissolution media to produce comparable results. The volume of the dissolution media was 20 ml.

The duration of dissolution tests was 72 h, and samples were taken at the following time points; 15 min, 60 min, 120 min, 240 min, 360 min, 24 h, 48 h, and 72 h. The sample volume was 1 ml, which was replaced by pure dissolution medium. For ARG-IND, however, preliminary studies revealed the need for adjusting the pH continuously. Hence, in order to have enough time to adjust the pH, the sampling frequency from ARG-IND PM and ARG-IND CA solutions was reduced (120 min, 360 min, 24 h and 72 h for ARG-IND PM and 15 min, 120 min, 360 min, 24 h and 72 h for co-amorphous ARG-IND). The samples were filtered immediately after sampling through a 0.22 μm membrane filter (Syringe Filter 30 mm Dia, PES 0.22 μm Membrane, Sterile, Porvair Sciences). In addition, preliminary studies indicated that IND tended to adsorb onto the filter material. This phenomenon was eliminated by filtering 3 ml of test solution (1 ml from each flask) through the filter prior to the first sample, and that same filter was used during the rest of the experiment.

2.4 Precipitation tests

Precipitation tests were conducted with the solvent shift method using DMSO as an organic solvent. DMSO was selected based on a 72 h solubility test, where IND was found to have the highest solubility in DMSO (499 ± 60 mg/ml) when compared to ACN (23 ± 1 mg/ml) and methanol (36 ± 0.4 mg/ml). The supersaturated state of IND was achieved by adding 2 % (V/V) (i.e. 400 µl in 20 ml) of DMSO-IND solution to the dissolution media.

An IND-DMSO solution was prepared for each medium. The IND concentration of the solution was set to produce four times the concentration reached with amorphous IND at the 72 h time point in each dissolution media. The theoretical maximum concentrations were 100 µg/ml in FeSSIF blank, 1900 µg/ml in FaSSIF blank, 480 µg/ml in FeSSIF, and 3300 µg/ml in FaSSIF. Prior to the study, the AAs were dissolved in FaSSIF blank, FeSSIF blank, FaSSIF, and FeSSIF in an amount corresponding to the molar ratio of 1:1 with the desired initial IND concentration, and 20 ml of those solutions were poured into Erlenmeyer flasks. 400 µl of IND-DMSO solution was then added to the precipitation test medium. Precipitation tests were performed under the same conditions and using the same equipment as in the dissolution tests. However, the sample volume was not replaced with pure medium.

2.5 High performance liquid chromatography (HPLC)

IND concentrations were measured by HPLC. The HPLC equipment consisted of Gilson 321 pump, Gilson UV-vis 151 detector (Both from: Gilson Inc., Middleton, WI, USA), Gilson 234 auto injector (Gilson, Roissy-en-France, France), and a reversed phase column (Phenomenex Gemini NX 5u C18 110A, 250x4,60 mm, sr. nr. 590531-19, USA) with a precolumn. The mobile phase flow rate was set to 1.2 ml/min and the detection wavelength to 225 nm. The mobile phase consisted of ACN (70 %), H_2O (30 %) and TFA (0.1 %). The results were analyzed using Gilson Unipoint software (version 3.01, Gilson Inc., Middleton, WI, USA).

The samples were diluted with ACN immediately after filtration to prevent precipitation and to produce an ACN/H_2O-ratio corresponding to the mobile phase (70/30). If necessary, the samples were diluted with more of the ACN/H_2O 70/30-mixture.

A series of standard solutions (100, 75; 50; 25; 12.5 and 0.5 µg/ml) was prepared in ACN/H_2O 70/30-mixture. The calibration curves were linear ($R^2 > 0,997$) in the abovementioned concentration range. The repeatability of the HPLC method was further evaluated by analyzing 5 samples from 1 µg/ml and 50 µg/ml standard solutions. The RSD of retention times were 0.28 % for 50 µg/ml and 0.24 % for 1 µg/ml standard solution, and of peak areas 2.30 % and 6.99 %, respectively.

2.6 Solid-state analysis

X-Ray Powder Diffractometry (XRPD) analysis was conducted with Bruker D8 Discover diffractometer (Bruker AXS GmbH, Karlsruhe, Germany) with Cu Kα radiation (λ = 1,54 Å). An acceleration voltage of 40 kV and a current of 40 mA were used. Samples were scanned between 5° and 35° 2θ using scan speed of 0.13° 2θ/s and a step size of 0.01°. DIFFRAC.V3 program (Bruker AXS GmbH, Karlsruhe, Germany) was used for data collection.

Thermo Nicolet Nexus 8700 spectrometer (Thermo Electron Corp, Madison, WI, USA) with attenuated total reflectance (ATR) accessory (Smart Endurance, Single reflection ATR diamond composite crystal) was used for Fourier Transform Infrared (FTIR) measurements. A total of 64 scans were recorded over a wave number range of 650-4000 nm (resolution 4 cm^{-1}) to collect each spectrum. OMNIC software (Thermo Nicolet Corp, Madison, WI, USA) was used for data collection.

Differential Scanning Calorimetry (DSC) measurements were conducted with a Mettler Toledo DSC 823^e (Mettler Toledo, Schwerzenbach, Switzerland) apparatus. Thermograms were obtained under a nitrogen gas flow of 50 ml/min. The sample powder (approx. 5 mg) was placed in an aluminum pan

with a pierced lid that was rapidly cooled down to -50 °C and kept there for 15 minutes. Then the temperature was raised at 10 °C/min until 180 °C was reached. STARe software (Mettler Toledo, Schwerzenbach, Switzerland) was used for data collection (T_g (midpoint) and melting temperature (T_m, onset)). All temperatures were calculated as a mean of three separate measurements.

2.7 Investigation of the precipitate originally formed in FeSSIF (pH 6.5)

The precipitate (unprocessed and after 60 min drying at 40 °C) from the IND-ARG PM dissolution test performed in FeSSIF (pH 6.5) was investigated with XRPD and FTIR (methods described in section 2.6) in order to determine its composition. Furthermore, ARG-IND PM was dissolved to pure water to reveal whether the precipitate could be formed without the components of FeSSIF. In addition, the preparation of pure crystalline ARG-IND-salt for reference was attempted by evaporating water from an ARG-IND aqueous solution (3.8 g ARG-IND PM in 5 ml of water) on a Petri dish under ambient conditions. Both the precipitate and the salt were investigated with FTIR and XRPD.

The precipitates from water and FeSSIF (pH 6.5) were investigated with DSC as described in 2.6. The precipitate samples were first cooled rapidly to -50 °C, maintaining the temperature at -50 °C for 15 min, and then the temperature was raised by 10 °C/min until 250 °C was reached. Alternatively, the moisture content of the sample was lowered by first increasing the temperature to 90 °C for 15 min after which the run was performed as described above.

Solid-state Nuclear Magnetic Resonance (ssNMR) spectrum was only collected from FeSSIF (pH 6.5) precipitate with Bruker Avance 400 MHz spectrometer (Bruker BioSpin GmbH, Rheinstetten, Germany) operating at a carbon Larmor frequency of 100.62 MHz. The CP/MAS experiment was carried out using a CP/MAS probehead and 4 mm ZrO_2 rotors. The sample was spun at a rate of 5 kHz. The number of scans collected at r.t. was ~42 k, CP contact time being 2 ms and the relaxation delay 4

s. The ^{13}C chemical shifts were calibrated using the carbonyl signal of a glycine sample at 176.5 ppm as an external standard.

2.8 Data analysis

GraphPad Prism 5.03 (GraphPad Software Inc., La Jolla, USA) was used to calculate areas under the curves (AUC) and perform statistical analysis. The AUCs of concentration-time profiles (from 0 to 72 h, AUC_{0-72}) from dissolution studies with crystalline material were calculated by linear trapezoidal integration to examine the effect of the AAs on IND dissolution as a physical mixture. The differences between AUC_{0-72}s were analyzed by one-way ANOVA with Tukey's Multiple Comparison Test as a post-hoc test.

The supersaturation in dissolution and precipitation studies was evaluated by the method introduced by Bevernage et al. [27]. Briefly, all dissolution data was plotted as degree of supersaturation (DS)-time profiles. With amorphous materials, DS was calculated by dividing the measured IND concentration by the IND equilibrium concentration (concentration of the 72 h sample obtained from the dissolution test with crystalline material) (Table 1) whereas in precipitation tests, the measured concentration was divided by the concentration of the 72 h amorphous IND sample (Table 1).

In addition, the AUCs of DS-time profiles (AUC_{DS}) were calculated, and they were then used to calculate supersaturation factors (SF) of IND and excipient gain factors (EGF) of AAs, as described by Bevernage et al. [27]. In the dissolution studies, the AUCs of the whole DS-time profile (AUC_{DS0-72}) were calculated whereas in precipitation studies only the values from the first 360 min were considered ($AUC_{DS0-360}$). The SFs were calculated by dividing the experimental AUC_{DS}s of IND in different media by the theoretical AUC_{DS} of IND at equilibrium concentration (DS=1), whereas when calculating the EGFs, the experimental AUC_{DS}s in the presence of AAs were divided by the experimental AUC_{DS} of plain IND. Hence, the SFs provide information on the supersaturation induced by amorphization in the

different media, and the EGFs illustrate the precipitation inhibitory effect (i.e. stabilization of the supersaturation) of the different AAs [27]. The EGFs were analyzed with one-way ANOVA with Dunnett's Multiple Comparison Test as a post-hoc test [27]. In addition, we compared the SFs in different media by one-way ANOVA with Tukey's Multiple Comparison Test. The results of all statistical analyses were considered statistically significant when $p < 0.05$.

3. RESULTS

3.1 Solid state analysis of the cryomilled materials

Based on the XRPD measurements (data not shown) all materials had fully transformed into their amorphous forms. Thermal analysis with DSC indicated that the co-amorphous AA-IND mixtures were homogenous mixtures, since only one glass transition was present in each thermogram. T_gs measured in this study; however, differed slightly from the values measured by Löbmann et al. (Table 2) [24]. According to FTIR spectra collected in this study (not shown here), the only interaction between AAs and IND seems to be the salt formation between ARG and IND, which is consistent with the report of Löbmann et al. [25].

3.2 Dissolution studies

3.2.1 AA-IND PMs and crystalline IND

There were notable and statistically significant variations in the equilibrium solubility (concentration in 72 h IND samples) of plain crystalline IND depending on the dissolution media (Figure 1, Table 1). The rank order of IND solubilities in different media was the same, namely FeSSIF blank < FeSSIF < FaSSIF blank < FaSSIF, regardless of the presence of amino acids.

Figure 1 provides evidence that ARG was the only AA capable of modifying the dissolution of IND as a physical mixture. This effect was observed in FaSSIF blank, FeSSIF, and FaSSIF where IND

concentrations were initially from 4 to 17 times higher in the presence of ARG than the IND equilibrium concentration in the corresponding media. In these media, also the AUC_{0-72} of the concentration-time profiles were statistically significantly higher in the presence of ARG (Table 3).

3.2.2 AA-IND CAs and amorphous IND

The concentration-time and DS-time profiles (Figure 2) of AA-IND CAs and amorphous IND revealed the clear IND supersaturation in the presence of ARG in FaSSIF blank and FaSSIF. In FeSSIF blank and FeSSIF, the effect was less obvious. In the majority of the tests, the dissolution profiles of the other co-amorphous mixtures were similar with amorphous IND. However, in FeSSIF blank, TRP seems to delay the precipitation of IND for the first 4 hours.

SFs (table 4) were determined in different dissolution media to evaluate the supersaturation caused by plain amorphous IND, and to establish the ability of biorelevant media to stabilize IND supersaturation. In both blank media and in FaSSIF, the mean of SFs were approximately 1.1, but in FeSSIF, it was slightly less than 1. According to the statistical analysis, there were significant differences in the SFs only between FaSSIF and FeSSIF.

The highest EGF-values (Figure 3) were observed with ARG-IND in FaSSIF blank (EGF ~ 3.4) and FaSSIF (EGF ~10.7). In other media and with the other AAs, the EGFs remained below 2. Nevertheless, statistically significant differences in the AUCs of DS-time profiles between AA-IND CAs and amorphous IND were observed in all of the dissolution media.

3.3 Precipitation studies

The DS-time profiles are presented in Figure 4. The profiles reveal that the desired initial IND concentration was achieved with all material combinations in FeSSIF blank, FaSSIF blank and FeSSIF. In FaSSIF, the intended initial degree of supersaturation (DS=4) was only observed in the presence of

ARG, which maintained that concentration throughout the experiment. In FaSSIF solutions with PHE and TRP, the IND concentration had decreased markedly already during the first 15 min, at that time point being less than 50 % of the desired initial concentration.

The Supersaturation factors calculated for IND (table 4) demonstrated that a clear supersaturation had been generated also without excipients in all media except FaSSIF. The supersaturation factors differed statistically significantly between FaSSIF and FaSSIF blank, and FaSSIF blank and FeSSIF blank, but no significant difference was observed between FeSSIF blank and FeSSIF.

The calculation of EGFs revealed that ARG was the only amino acid with a statistically significant ability to inhibit IND precipitation, and this inhibition was only observed in FaSSIF blank and FaSSIF (Figure 5). With PHE and TRP, no precipitation inhibition was observed in any media. In fact, in FeSSIF blank, the excipient gain factors of all amino acids remained below 1 ($p < 0.05$), which suggests that the $AUC_{DS0\text{-}360}$ was actually higher with plain IND than in the presence of amino acids.

3.4 Investigation of the ARG-IND precipitate

Adding excess ARG-IND PM to FeSSIF (pH 6.5) produced a yellowish, moist precipitate, which filled the entire volume of the original solution, i.e. no separate solution phase could be observed. Figure 6 presents the diffractogram of this precipitate. The diffractogram of the precipitate prepared similarly from pure water and the diffractogram of ARG-IND salt prepared by dissolving ARG-IND PM in water and then slowly evaporating the water are shown for comparison. In addition, the diffractograms of crystalline IND, crystalline ARG and ARG-IND PM are presented. The lack of diffraction peaks in the diffractogram of ARG-IND salt (water evaporated) reveals that we had been unable to produce the crystalline ARG-IND salt even by slowly evaporating the water. On the other hand, the peaks in the diffractograms of all the other precipitates indicate that there was crystalline material present.

The diffractograms of all the precipitates are similar regardless of the media from which they had been precipitated. Additionally, all the peaks that could be found in the diffractograms of the undried precipitates were also present in the diffractograms of the dried samples, although drying revealed some new diffraction peaks. The only peaks in the diffractogram of dried precipitate that seemed to originate clearly from either ARG or IND, were the peaks at 2θ-value of 15.8° (15.6° and 15.7° in the diffractograms of IND and ARG-IND PM respectively) and 18.3° (18.2° in the ARG and ARG-IND PM diffractograms). Additionally, peaks at 2θ-values of 19.2°, 19.9°, 20.3°, and 21.3° in the diffractograms of dried precipitates were close to the peaks in the diffractograms of either ARG or IND or both, but the large amount of peaks complicated their interpretation.

The unique features in the diffractograms of the precipitates were more readily observed; these included the lack of peaks below 2θ-value of 13° and the emergence of peaks at 2θ-values of 13.1° (invisible with undried precipitate) and 14.1° (14.0° for undried precipitate). Furthermore, peaks at 2θ-values of 17.6°, 18.8°, 22.3°, and 23.4° in the precipitate diffractograms were missing from the diffractograms of ARG, IND, and ARG-IND PM. These features were also absent from the diffractograms of other IND polymorphs, except for the α-IND diffraction peak at 14.0° 2θ [28]. Some similarities were, however, found between the diffractograms of precipitates and indomethacin sodium salts (IND-Na anhydrate: 13.3° 2θ, IND-Na trihydrate: 17.75°, 19.4°, and 21.38 ° 2θ), but since the same precipitate was formed also from pure water (without the presence of sodium ions), this salt formation was excluded [29-31].

Regardless of drying or the medium used, all the precipitates exhibited similar FTIR-spectra, which, however, differed from the spectra of crystalline ARG, γ-IND, amorphous IND, ARG-IND PM and ARG-IND CA (Figure 7). The FTIR-spectrum of the salt produced by slow evaporation was nearly

identical to the spectrum of ARG-IND CA, which confirmed that a co-amorphous product was formed with this method.

The most significant differences between the IR spectrum of ARG-IND CA and the IR spectra of crystalline ARG and amorphous IND were observed between wave-numbers of 1500 and 1750 cm^{-1}, i. e. a plateau was formed in ARG-IND CA. The major differences between the spectra of the precipitates and spectra of the other materials were also observed in this region, but the wide plateau of the co-amorphous mixture was absent. Instead a sharp peak at 1678 cm^{-1} (originating probably from asymmetric stretches of ARG guanidyl- and COO^{-}groups) and a broad peak (formed probably by several overlapping peaks) with a sharper tip at 1580 cm^{-1} could be detected for the precipitates [25]. The absence of peaks between 1700 and 1725 cm^{-1} in the precipitate spectra suggested that the COOH-groups of IND had become ionized, evidence of salt formation [25]. Due to the broad, overlapping peak at 1580 cm^{-1}, the vibrations of ionized COO^{-}groups of IND (usually between 1505 and 1610 cm^{-1}) remained unidentified [25]. The wave-number region from 1300 to 1500 cm^{-1} was similar between the precipitate spectrum and the spectra of amorphous IND and ARG-IND CA. However, the precipitate spectrum included a divided peak (1320 and 1307 cm^{-1}) instead of single peak at 1316 cm^{-1}(amorphous IND) or at 1321 cm^{-1}(ARG-IND CA). From 1200 to 1300 cm^{-1} the precipitate spectrum contained six partly overlapping peaks while the spectra of other materials exhibited a maximum of three peaks in that area. The remaining wave-number area under examination (from 1000 to 1200 cm^{-1}) was similar between precipitate and amorphous IND and ARG-IND CA except for the divided peak in the precipitate spectrum (1150 and 1139 cm^{-1}) compared to the single peak at 1146 (amorph IND) or 1147 cm^{-1} (ARG-IND CA).

The thermograms of the precipitates produced by two DSC methods are presented in Figure S1. The most interesting feature in the thermograms of the precipitates was the endothermic peak, whose

position ranged from 191 to 211 °C depending on the precipitation media and DSC method. This peak was present in the thermograms of precipitates from both FeSSIF (pH 6.5) and water, it was visible with both DSC methods (with and without drying phase), and the position of the endotherm was close to the melting temperature of recrystallized ARG-IND salt (209.73 °C) [32]. Another significant endotherm was detected at 158 °C in the thermogram of precipitate from FeSSIF (pH 6.5) (without drying phase), which implies that there may have been crystalline IND left (we measured the melting temperature of recrystallized indomethacin to be approximately 159 °C). In addition to the abovementioned endotherms, a wide endothermic peak (onset temperature ranging from 64 to 104 °C) was present in the thermograms of most of the precipitate samples. This peak, however, seemed to relate to the moisture content of the samples, since it was smaller or totally absent in the thermograms of dried precipitates.

The ssNMR measurements were only performed for the original precipitate from the FeSSIF (pH 6.5). The ssNMR spectrum of the precipitate contained many of the resonances, which were present in the spectrum of pure γ-IND (19.5, 61.9, 111.5, 120.3, 125.2, 137.4-144.6, 162.0, 174.0, and 180.0 ppm). The divided peaks in the spectrum at 161.4-162.9 ppm and 180.8-185.3 ppm, may have originated from resonances of both ARG and IND, but otherwise the signals from the crystalline ARG were not visible. This, however, may have been due to overlapping of IND and ARG peaks. The ssNMR results thus suggested that the precipitate consisted of ARG and IND. Furthermore, the ^{13}C chemical shift of the carboxylate of ARG appearing at >182 ppm indicated ionization, supporting the FTIR result of salt formation. As mentioned by Jensen et al., though, the observation of salt formation between ARG and IND with ssNMR was challenging due to the presence overlapping resonances [33]. It was noteworthy, however, that the ssNMR spectrum of ARG-IND CA reported by Jensen et al. resembled the current spectrum of the precipitate, except that the peaks in the ARG-IND CA spectrum were broader, which is

typical of an amorphous material [33,34]. The narrower peaks in the current spectrum were indicative of the more crystalline nature of the precipitate.

4. DISCUSSION

In the present study, we performed dissolution studies in biorelevant media (FaSSIF, FeSSIF) with co-amorphous AA-IND mixtures, which have previously been shown to improve the stability and the intrinsic dissolution rate of amorphous indomethacin. The main aim was to investigate whether the AAs would be able to prolong the possible supersaturation caused by amorphous indomethacin. Additionally, we performed precipitation studies to determine whether the co-amorphization plays any role in stabilizing the supersaturated state in biorelevant conditions.

The results obtained from the FTIR and XRPD measurements of co-amorphous AA-IND mixtures prepared by cryomilling were very similar to the results reported by Löbmann et al., which suggests that as long as the milling temperature is kept low, either by cryomilling or by milling in a cold room, the end product is amorphous, and the interactions between molecules remain similar [24,25]. Different preparation methods and even the same methods with different conditions, however, have been shown to affect structural and thermal properties (such as T_g) of amorphous IND, and these may account for the differences between the T_gs of ball milled and cryomilled materials [24,25,35,36].

The equilibrium solubility of crystalline IND differed significantly between dissolution media (Figure 1), which can be explained by the variations in pH and the bile salt and phospholipid concentrations. IND is a weak acid with a pK_a value of 4.5, which means that at pH 6.5 (FaSSIF blank and FaSSIF) many more IND molecules is in the ionized form than at pH 5.0, and thereby the solubility is increased [37]. In addition, the solubility of IND was markedly higher in the biorelevant media when compared to the corresponding blank buffers. This difference can be explained by the solubilizing effect of the biorelevant medium components, which, however, seems to be outweighed by the effect of pH since

the IND solubility in FaSSIF blank was significantly higher than in FeSSIF [38]. Additionally, the solubilizing effect appeared to be more pronounced in pH 5.0, which may be explained by the higher surfactant concentration, and the fact that the unionized (and more lipophilic) form of the drug partitions more readily into micelles than its ionized form [39].

It was crucial to evaluate the effect of ARG, PHE, and TRP on IND dissolution already as a physical mixture in order to understand the mechanism through which these amino acids could possibly inhibit precipitation when they were formulated in the co-amorphous form. After the dissolution experiment, it was evident that PHE and TRP were unable to affect the dissolution of IND. ARG, however, caused a significant increase in the initial IND concentration in FaSSIF blank, FeSSIF and FaSSIF. The ability of ARG to increase IND concentrations as a physical mixture or freely in a solution has also been observed by ElShaer et al., Lenz et al., and Qi et al. [32,40,41]. Possible explanations for the solubilizing effect of ARG include the acidic nature of IND and alkaline nature of ARG (i.e. salt formation), an interaction between the guanidinium group of ARG and the aromatic groups of IND, and an ARG dependent *in situ* amorphization of IND [32,40-42]. In this study, the pH increasing effect of ARG was excluded by adjusting the pH prior to every sample, evidence that at least in FaSSIF blank and FaSSIF, ARG might have acted as a counter ion and caused IND dissociation as described by ElShaer et al. [32]. The *in situ* amorphization and the subsequent formation of an amorphous ARG-IND salt are also a possible solubilisation mechanism since the clear supersaturation occurred before reaching the plateau. It may, however, only apply in FeSSIF, since Lenz et al. reported that *in situ* amorphization was observed at pH 4.5 but not at pH 6.8 [40].

In the present study, ARG-IND CA was the only amorphous material that produced clearly supersaturated IND concentrations. This supersaturation was most obvious in FaSSIF blank and FaSSIF, but EGFs show a statistically significant effect also in other media. The significant effect of

ARG could be expected from three sources; 1) the results of dissolution tests with crystalline material, 2) the major intrinsic dissolution rate increases described in the studies of Löbmann et al. and Jensen et al., and 3) the supersaturation already observed by Lenz et al. [24,40,43]. The highest supersaturation maintained by ARG in FaSSIF blank and FaSSIF was probably due to the higher pH, which led to the ionization of IND, promoting electrostatic interactions with ARG [32]. At pH of 5.0, the salt formation probably played only a minor role, and the supersaturation stabilization may have been due to the solubilizing effect caused by interactions between the guanidinium group of ARG and the aromatic moiety of IND. The relatively modest DSs in FeSSIF compared to FeSSIF blank could be explained by the major solubilizing effects of bile salts and phospholipids, which could outweigh the supersaturation effect as was observed in a study with a co-amorphous mixture of simvastatin and lysine, although with ARG-IND PM, clear evidence of supersaturation was observed also in FeSSIF [44].

No specific interactions between molecules (e.g. salt formation) were identified in PHE-IND CA or TRP-IND CA, which most likely explains the less significant effect of PHE and TRP on IND supersaturation [25]. In addition, the lower intrinsic dissolution rates noted in the study of Löbmann et al. indicated that these excipients exerted only minor effects on IND dissolution and its possible supersaturation [24]. It is, however, noteworthy that with TRP, the EGFs revealed a statistically significant effect on IND supersaturation in every medium except FaSSIF, whereas neither PHE nor TRP exerted any negative effect on IND dissolution or supersaturation. The low SFs indicate the absence of supersaturation also with pure amorphous IND, and despite the slight statistically significant differences in SFs between different media, it seems that the components of the biorelevant media are virtually unable to maintain IND supersaturation.

As far as we are aware, this is the first time that the ability of amino acids to prevent precipitation from supersaturated solution generated by co-amorphous system has been compared to the ability of amino acids freely in solution to inhibit precipitation of a drug. As in dissolution tests with amorphous

materials, the effect of ARG was most significant in FaSSIF blank and FaSSIF where no precipitation occurred. In other media, ARG had no significant effect on IND precipitation; this was also the case with the other tested AAs in any media (EGFs~1). This result indicates that it is the interactions formed during the preparation of co-amorphous mixtures that are responsible for the inhibitory effect (although modest) of PHE and TRP (and ARG at low pH) on IND precipitation. Here again the effect of ARG to prevent precipitation was shown to be pH dependent, which may be explained by the higher IND solubility increase achieved by ARG at pH 6.5. The mechanism behind this solubility increase is probably related to the IND ionization and the subsequent salt formation between IND and ARG.

The non-significant difference between IND SFs in precipitation tests performed in FeSSIF blank and FeSSIF suggests that the biorelevant components had been unable to inhibit precipitation of IND. In fact, the present results indicate that at higher pH-values, precipitation may happen even more quickly in the presence of bile salts and phospholipids ($SF_{FaSSIF} < SF_{FaSSIF\ blank}$). Our finding is consistent with the work of Bevernage et al. who observed that the supersaturation measured with three model drugs was more stable in FaSSIF blank than FaSSIF [45]. This was attributed to the increased solubility in FaSSIF, which increases the amount of intermolecular collisions and the possibility of nucleation. In FeSSIF, the indomethacin concentrations may have remained sufficiently low to avoid the increased nucleation even though the concentration was many times higher than in the FeSSIF blank. However, despite the less stable supersaturation, the IND concentration remained higher in both the FaSSIF blank and FaSSIF than in FeSSIF throughout the experiment.

During the investigation of the composition of the ARG-IND precipitate, we discovered that the precipitation was independent of the media composition, which we interpreted that the precipitate consisted of only ARG or IND or both. The diffraction peaks in the diffractogram suggest that the precipitate was at least partly crystalline, but since the diffractogram differed from the diffractograms of γ-IND, other IND polymorphs, crystalline ARG and ARG-IND PM, one must conclude that the

precipitate was not simply a physical mixture of crystalline components. The changes in the FTIR spectra also implied that ARG and IND had interacted to produce the precipitate. Since ARG is basic and IND is acidic, there were no free carboxyl groups vibrating in the FTIR spectrum, and the salt formation between the molecules is well-established, we assume that the precipitate was a crystalline salt of ARG and IND with possible residual IND and ARG [25,32]. This conclusion was further confirmed by the DSC and ssNMR measurements, where melting endotherms close to the value of recrystallized ARG-IND salt, and NMR shifts consistent with salt formation were detected. Although salt formation between ARG and IND has been shown to occur as a result of spray drying, ball milling, and freeze drying, as far as we are aware, this is the first time that the formation of crystalline ARG-IND salt has been reported [25,32,43].

5. CONCLUSIONS

The main aim of this study was to investigate the ability of AAs to stabilize the supersaturated state when they are formulated as co-amorphous mixtures with a drug. All of the three AAs examined in this study were able, at least slightly, to stabilize IND supersaturation, but the extent of stabilization was highly dependent on the media and the interactions between the AA and drug molecules. However, the precipitation tests demonstrated that the formation of co-amorphous mixtures improved the ability of AAs to prevent precipitation. This information combined with the improved stability, makes the drug-AA co-amorphous mixtures an interesting option for exploring when formulating poorly soluble drugs [24].

ACKNOWLEDGMENT

RO acknowledges the support from the Doctoral Programme in Drug Research in the Doctoral School of University of Eastern Finland.

APPENDIX

Supplementary data associated with this article can be found in the online version.

REFERENCES

[1] A. Glomme, J. März, J.B. Dressman, Predicting the Intestinal Solubility of Poorly Soluble Drugs, in Pharmacokinetic Profiling in Drug Research, 2007, pp. 259-280.

[2] C.A. Lipinski, Drug-like properties and the causes of poor solubility and poor permeability, J. Pharmacol. Toxicol. Methods 44 (2000) 235-249. doi: 10.1016/S1056-8719(00)00107-6.

[3] C.A. Lipinski, F. Lombardo, B.W. Dominy, P.J. Feeney, Experimental and computational approaches to estimate solubility and permeability in drug discovery and development settings, Adv. Drug Deliv. Rev. 46 (2001) 3-26. doi: 10.1016/S0169-409X(00)00129-0.

[4] T. Takagi, C. Ramachandran, M. Bermejo, S. Yamashita, L.X. Yu, G.L. Amidon, A provisional biopharmaceutical classification of the top 200 oral drug products in the United States, Great Britain, Spain, and Japan, Mol. Pharm. 3 (2006) 631-643. doi: 10.1021/mp0600182.

[5] J.B. Dressman, M. Vertzoni, K. Goumas, C. Reppas, Estimating drug solubility in the gastrointestinal tract, Adv. Drug Deliv. Rev. 59 (2007) 591-602. doi: 10.1016/j.addr.2007.05.009.

[6] P. Augustijns, B. Wuyts, B. Hens, P. Annaert, J. Butler, J. Brouwers, A review of drug solubility in human intestinal fluids: implications for the prediction of oral absorption, Eur. J. Pharm. Sci. 57 (2014) 322-332. doi: 10.1016/j.ejps.2013.08.027.

[7] H. Lennernas, B. Abrahamsson, The use of biopharmaceutic classification of drugs in drug discovery and development: current status and future extension, J. Pharm. Pharmacol. 57 (2005) 273-285. doi: 10.1211/0022357055263.

[8] C.W. Pouton, Formulation of poorly water-soluble drugs for oral administration: physicochemical and physiological issues and the lipid formulation classification system, Eur. J. Pharm. Sci. 29 (2006) 278-287. doi: 10.1016/j.ejps.2006.04.016.

[9] S.B. Murdande, M.J. Pikal, R.M. Shanker, R.H. Bogner, Solubility advantage of amorphous pharmaceuticals: I. A thermodynamic analysis, J. Pharm. Sci. 99 (2010) 1254-1264. doi: 10.1002/jps.21903.

[10] S.B. Murdande, M.J. Pikal, R.M. Shanker, R.H. Bogner, Solubility advantage of amorphous pharmaceuticals, part 3: Is maximum solubility advantage experimentally attainable and sustainable?, J. Pharm. Sci. 100 (2011) 4349-4356. doi: 10.1002/jps.22643.

[11] B.C. Hancock, M. Parks, What is the true solubility advantage for amorphous pharmaceuticals?, Pharm. Res. 17 (2000) 397-404. doi: 10.1023/A:1007516718048.

[12] R. Laitinen, K. Lobmann, C.J. Strachan, H. Grohganz, T. Rades, Emerging trends in the stabilization of amorphous drugs, Int. J. Pharm. 453 (2013) 65-79. doi: 10.1016/j.ijpharm.2012.04.066.

[13] J.M. Miller, A. Beig, R.A. Carr, J.K. Spence, A. Dahan, A win-win solution in oral delivery of lipophilic drugs: supersaturation via amorphous solid dispersions increases apparent solubility without sacrifice of intestinal membrane permeability, Mol. Pharm. 9 (2012) 2009-2016. doi: 10.1021/mp300104s.

[14] J.M. Miller, A. Beig, R.A. Carr, G.K. Webster, A. Dahan, The solubility-permeability interplay when using cosolvents for solubilization: revising the way we use solubility-enabling formulations, Mol. Pharm. 9 (2012) 581-590. doi: 10.1021/mp200460u.

[15] J.M. Miller, A. Beig, B.J. Krieg, R.A. Carr, T.B. Borchardt, G.E. Amidon, G.L. Amidon, A. Dahan, The solubility-permeability interplay: mechanistic modeling and predictive application of the impact of micellar solubilization on intestinal permeation, Mol. Pharm. 8 (2011) 1848-1856. doi: 10.1021/mp200181v.

[16] Y. He, C. Ho, Amorphous Solid Dispersions: Utilization and Challenges in Drug Discovery and Development, J. Pharm. Sci. 104 (2015) 3237-3258. doi: 10.1002/jps.24541.

[17] S. Baghel, H. Cathcart, N.J. O'Reilly, Polymeric Amorphous Solid Dispersions: A Review of Amorphization, Crystallization, Stabilization, Solid-State Characterization, and Aqueous Solubilization of Biopharmaceutical Classification System Class II Drugs, J. Pharm. Sci. 105 (2016) 2527-2544. doi: 10.1016/j.xphs.2015.10.008.

[18] H.R. Guzman, M. Tawa, Z. Zhang, P. Ratanabanangkoon, P. Shaw, C.R. Gardner, H. Chen, J.P. Moreau, O. Almarsson, J.F. Remenar, Combined use of crystalline salt forms and precipitation inhibitors to improve oral absorption of celecoxib from solid oral formulations, J. Pharm. Sci. 96 (2007) 2686-2702. doi: 10.1002/jps.20906.

[19] S.J. Dengale, H. Grohganz, T. Rades, K. Lobmann, Recent advances in co-amorphous drug formulations, Adv. Drug Deliv. Rev. 100 (2016) 116-125. doi: 10.1016/j.addr.2015.12.009.

[20] K. Lobmann, R. Laitinen, H. Grohganz, K.C. Gordon, C. Strachan, T. Rades, Coamorphous drug systems: enhanced physical stability and dissolution rate of indomethacin and naproxen, Mol. Pharm. 8 (2011) 1919-1928. doi: 10.1021/mp2002973.

[21] S. Wairkar, R. Gaud, Co-Amorphous Combination of Nateglinide-Metformin Hydrochloride for Dissolution Enhancement, AAPS PharmSciTech (2015) doi: 10.1208/s12249-015-0371-4.

[22] K.T. Jensen, K. Lobmann, T. Rades, H. Grohganz, Improving co-amorphous drug formulations by the addition of the highly water soluble amino Acid, proline, Pharmaceutics 6 (2014) 416-435. doi: 10.3390/pharmaceutics6030416.

[23] R. Laitinen, K. Lobmann, H. Grohganz, C. Strachan, T. Rades, Amino acids as co-amorphous excipients for simvastatin and glibenclamide: physical properties and stability, Mol. Pharm. 11 (2014) 2381-2389. doi: 10.1021/mp500107s.

[24] K. Lobmann, H. Grohganz, R. Laitinen, C. Strachan, T. Rades, Amino acids as co-amorphous stabilizers for poorly water soluble drugs--Part 1: preparation, stability and dissolution enhancement, Eur. J. Pharm. Biopharm. 85 (2013) 873-881. doi: 10.1016/j.ejpb.2013.03.014.

[25] K. Lobmann, R. Laitinen, C. Strachan, T. Rades, H. Grohganz, Amino acids as co-amorphous stabilizers for poorly water-soluble drugs--Part 2: molecular interactions, Eur. J. Pharm. Biopharm. 85 (2013) 882-888. doi: 10.1016/j.ejpb.2013.03.026.

[26] S.Y. Fong, A. Ibisogly, A. Bauer-Brandl, Solubility enhancement of BCS Class II drug by solid phospholipid dispersions: Spray drying versus freeze-drying, Int. J. Pharm. 496 (2015) 382-391. doi: 10.1016/j.ijpharm.2015.10.029.

[27] J. Bevernage, T. Forier, J. Brouwers, J. Tack, P. Annaert, P. Augustijns, Excipient-mediated supersaturation stabilization in human intestinal fluids, Mol. Pharm. 8 (2011) 564-570. doi: 10.1021/mp100377m.

[28] S.A. Surwase, J.P. Boetker, D. Saville, B.J. Boyd, K.C. Gordon, L. Peltonen, C.J. Strachan, Indomethacin: new polymorphs of an old drug, Mol. Pharm. 10 (2013) 4472-4480. doi: 10.1021/mp400299a.

[29] P. Tong, G. Zografi, Effects of water vapor absorption on the physical and chemical stability of amorphous sodium indomethacin, AAPS PharmSciTech 5 (2004) e26. doi: 10.1208/pt050226.

[30] A. Siddiqui, Z. Rahman, S.R. Khan, D. Awotwe-Otoo, M.A. Khan, Root cause evaluation of particulates in the lyophilized indomethacin sodium trihydrate plug for parenteral administration, Int. J. Pharm. 473 (2014) 545-551. doi: 10.1016/j.ijpharm.2014.07.035.

[31] A. Dubbini, R. Censi, V. Martena, E. Hoti, M. Ricciutelli, L. Malaj, P. Di Martino, Influence of pH and method of crystallization on the solid physical form of indomethacin, Int. J. Pharm. 473 (2014) 536-544. doi: 10.1016/j.ijpharm.2014.07.030.

[32] A. ElShaer, S. Khan, D. Perumal, P. Hanson, A.R. Mohammed, Use of amino acids as counterions improves the solubility of the BCS II model drug, indomethacin, Curr. Drug Deliv. 8 (2011) 363-372. doi: 10.2174/156720111795767924.

[33] K.T. Jensen, F.H. Larsen, K. Lobmann, T. Rades, H. Grohganz, Influence of variation in molar ratio on co-amorphous drug-amino acid systems, Eur. J. Pharm. Biopharm. (2016) doi: S0939-6411(16)30231-4 [pii].

[34] K.T. Jensen, F.H. Larsen, C. Cornett, K. Lobmann, H. Grohganz, T. Rades, Formation Mechanism of Coamorphous Drug-Amino Acid Mixtures, Mol. Pharm. 12 (2015) 2484-2492. doi: 10.1021/acs.molpharmaceut.5b00295.

[35] P. Karmwar, K. Graeser, K.C. Gordon, C.J. Strachan, T. Rades, Investigation of properties and recrystallisation behaviour of amorphous indomethacin samples prepared by different methods, Int. J. Pharm. 417 (2011) 94-100. doi: 10.1016/j.ijpharm.2010.12.019.

[36] P. Karmwar, J.P. Boetker, K.A. Graeser, C.J. Strachan, J. Rantanen, T. Rades, Investigations on the effect of different cooling rates on the stability of amorphous indomethacin, Eur. J. Pharm. Sci. 44 (2011) 341-350. doi: 10.1016/j.ejps.2011.08.010.

[37] National Center for Biotechnology Information., PubChem Compound Database; CID=3715, https://pubchem.ncbi.nlm.nih.gov/compound/3715 (Assessed Aug. 5, 2016).

[38] K. Kleberg, J. Jacobsen, A. Müllertz, Characterising the behaviour of poorly water soluble drugs in the intestine: Application of biorelevant media for solubility, dissolution and transport studies, J. Pharm. Pharmacol. 62 (2010) 1656-1668. doi: 10.1111/j.2042-7158.2010.01023.x.

[39] P. Sinko, Colloids, in Martin's Physical Pharmacy and Pharmaceutical Sciences: Physical, Chemical, and Biopharmaceutical Principles in the Pharmaceutical Sciences, 5th ed., Lippincott Williams & Wilkins, Baltimore, 2006, pp. 469-498.

[40] E. Lenz, K.T. Jensen, L.I. Blaabjerg, K. Knop, H. Grohganz, K. Lobmann, T. Rades, P. Kleinebudde, Solid-state properties and dissolution behaviour of tablets containing co-amorphous indomethacin-arginine, Eur. J. Pharm. Biopharm. 96 (2015) 44-52. doi: 10.1016/j.ejpb.2015.07.011.

[41] X. Qi, J. Zhang, W. Wang, D. Cao, Solubility and stability of indomethacin in arginine-assisted solubilization system, Pharm. Dev. Technol. 18 (2013) 852-855. doi: 10.3109/10837450.2011.595797.

[42] A. Hirano, T. Kameda, D. Shinozaki, T. Arakawa, K. Shiraki, Molecular dynamics simulation of the arginine-assisted solubilization of caffeic acid: intervention in the interaction, J Phys Chem B 117 (2013) 7518-7527. doi: 10.1021/jp401609p.

[43] K.T. Jensen, L.I. Blaabjerg, E. Lenz, A. Bohr, H. Grohganz, P. Kleinebudde, T. Rades, K. Lobmann, Preparation and characterization of spray-dried co-amorphous drug-amino acid salts, J. Pharm. Pharmacol. (2015) doi: 10.1111/jphp.12458.

[44] A.T. Heikkinen, L. DeClerck, K. Lobmann, H. Grohganz, T. Rades, R. Laitinen, Dissolution properties of co-amorphous drug-amino acid formulations in buffer and biorelevant media, Pharmazie 70 (2015) 452-457. doi: 10.1691/ph.2015.4210.

[45] J. Bevernage, J. Brouwers, S. Clarysse, M. Vertzoni, J. Tack, P. Annaert, P. Augustijns, Drug supersaturation in simulated and human intestinal fluids representing different nutritional states, J. Pharm. Sci. 99 (2010) 4525-4534. doi: 10.1002/jps.22154.

List of figures and tables

Tables

Table 1. Indomethacin (IND) concentrations in 72 h samples from dissolution tests performed with crystalline ($C_{72\ cryst}$) and with amorphous ($C_{72\ amorph}$) IND without amino acids.

Table 2. Glass transition temperatures (T_gs) of the co-amorphous arginine-indomethacin (ARG-IND), phenylalanine-indomethacin (PHE-IND), and tryptophan-indomethacin (TRP-IND) mixtures and amorphous IND measured in the present study and in the study by Löbmann et al. [24].

Table 3. The areas under the concentration-time curve from 0 to 72 h (AUC_{0-72}; mean ± SD) for physical mixtures of arginine and indomethacin (ARG-IND), phenylalanine and indomethacin (PHE-IND), and tryptophan and indomethacin (TRP-IND), and for plain crystalline indomethacin (IND) in pH 5.0 acetate buffer (FeSSIF blank), pH 6.5 phosphate buffer (FaSSIF blank), pH 5.0 fed state simulated intestinal fluid (FeSSIF) and pH 6.5 fasted state simulated intestinal fluid (FaSSIF). Statistically significant differences between AUCs of physical mixtures and pure IND are marked with an asterisk.

Table 4. The supersaturation factors (Mean ± SD) calculated from dissolution tests with amorphous indomethacin (SF_{DISSO}) and from precipitation tests with plain indomethacin (SF_{PRECIP}) in different media.

Figures

Fig 1. Concentration (Mean ± Standard deviation)-time profiles of crystalline indomethacin (IND cryst) and physical mixtures of arginine and indomethacin (ARG-IND PM), phenylalanine and indomethacin (PHE-IND PM), and tryptophan and indomethacin (TRP-IND PM) in A FeSSIF blank, B FaSSIF blank, C FeSSIF, and D FaSSIF.

Fig 2. The concentration-time profiles with the magnification from the first 6 hours (Mean ± Standard deviation) of co-amorphous amino acid-indomethacin mixtures (AA-IND CAs) and amorphous IND in A FeSSIF blank, B FaSSIF blank, C FeSSIF, and D FaSSIF. The degree of supersaturation is provided in the vertical axis on the right.

Fig 3. Excipient gain factors (Mean ± Standard deviation) for co-amorphous arginine-indomethacin (ARG-IND), phenylalanine-indomethacin (PHE-IND) and tryptophan-indomethacin (TRP-IND) in different dissolution media. Statistically significant differences based on comparison of AUC_{DS0-72}s between co-amorphous amino acid-indomethacin mixtures and amorphous indomethacin are marked with an asterisk.

Fig 4. Degree of supersaturation (DS)-time profiles of plain indomethacin (IND) or of IND in the presence of arginine (ARG), phenylalanine (PHE) or tryptophan (TRP) obtained from precipitation tests performed in A FeSSIF blank, B FaSSIF blank, C FeSSIF, and D FaSSIF. DSs are presented as Mean ± Standard deviation.

Fig 5. Excipient gain factors (Mean ± Standard deviation) of arginine, phenylalanine and tryptophan (ARG, PHE, and TRP, respectively) in different media. Statistically significant inhibition of precipitation based on comparison of $AUC_{DS0-360s}$ between amino acid-indomethacin combinations and pure indomethacin are marked with an asterisk.

Fig 6. The X-ray diffractograms for physical mixture of arginine and indomethacin (ARG-IND PM), crystalline ARG, γ-IND, ARG-IND salt produced by slowly evaporating solvent water (ARG-IND salt (water evaporated)), and either dried or undried ARG-IND precipitates from two different media (see subscripts).

Fig 7. The FTIR-spectra for amorphous indomethacin (IND), arginine (ARG)-IND salt produced by slowly evaporating solvent water (ARG-IND salt (water evaporated)), co-amorphous mixture of ARG and IND (ARG-IND CA), physical mixture of ARG and IND (ARG-IND PM), crystalline ARG, γ-IND, and either dried or undried ARG-IND precipitates from two different media (see subscripts).

Supplementary data

Fig S1. The thermograms of arginine-indomethacin mixtures precipitated from different media (see subscripts). Thermograms from DSC runs with and without drying phase (15 min in 90 °C) are included.

Fig S2. ssNMR spectrum of the mixture of arginine and indomethacin precipitated from FeSSIF (pH 6.5).

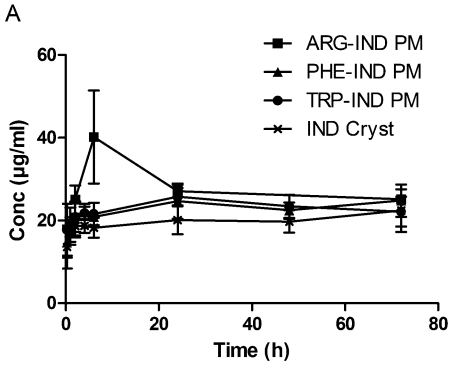

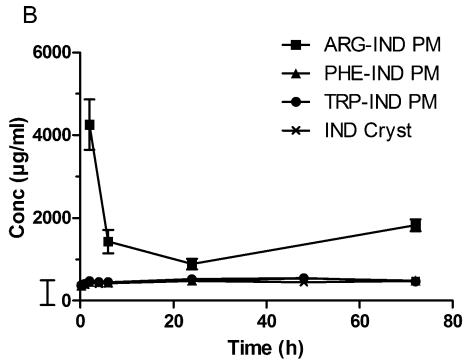

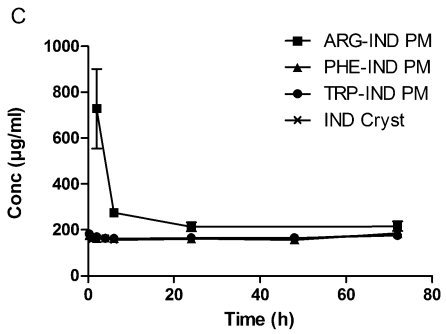

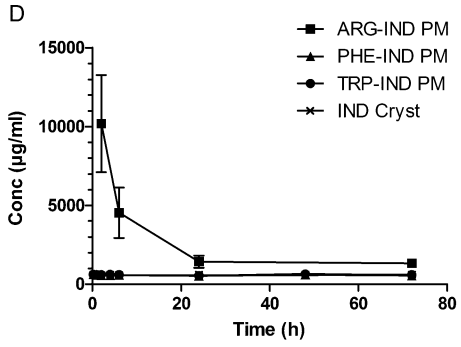

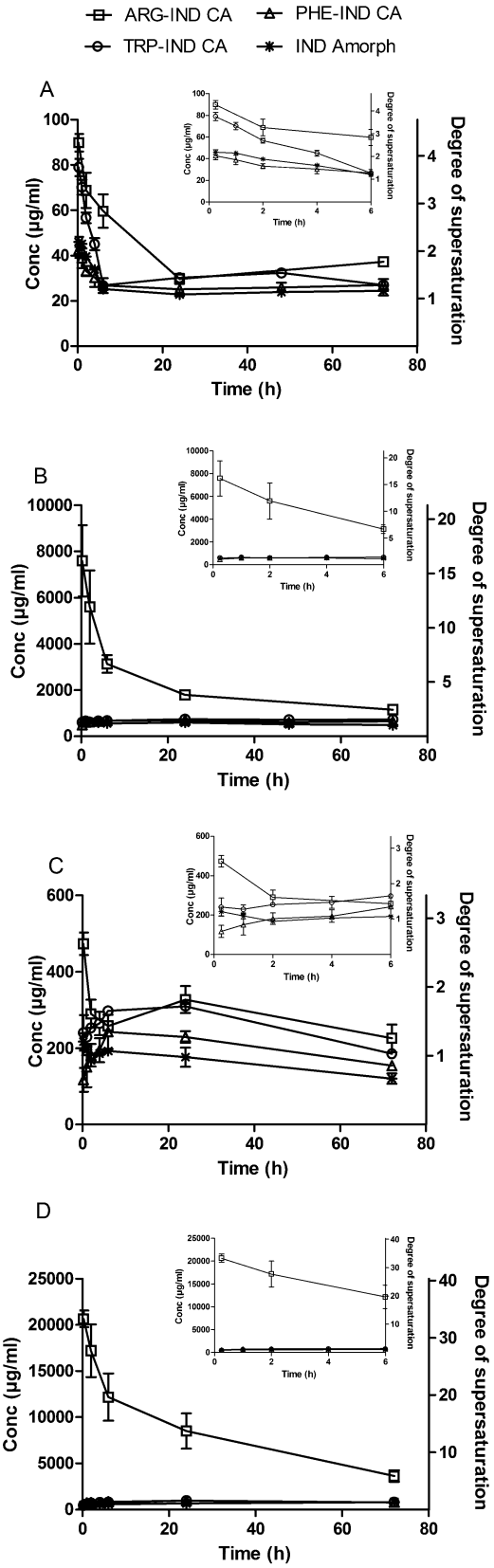

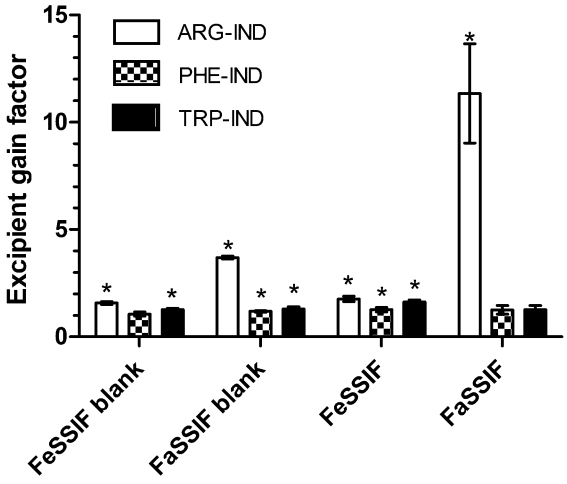

A

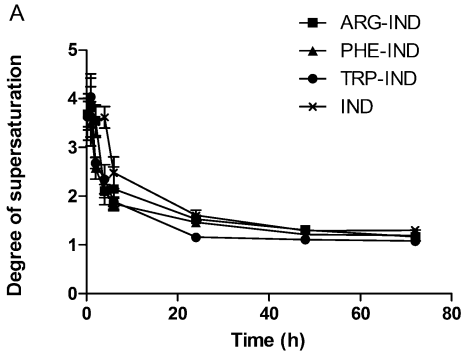

B

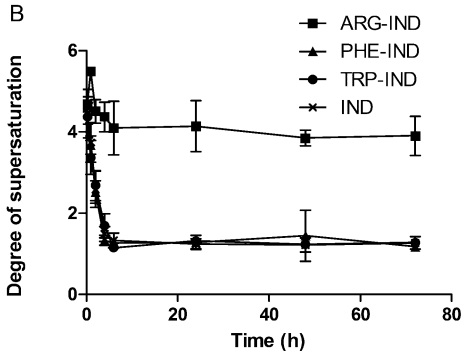

C

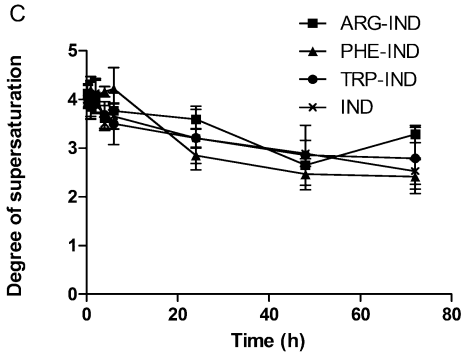

D

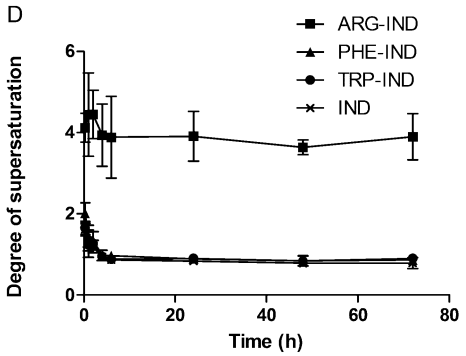

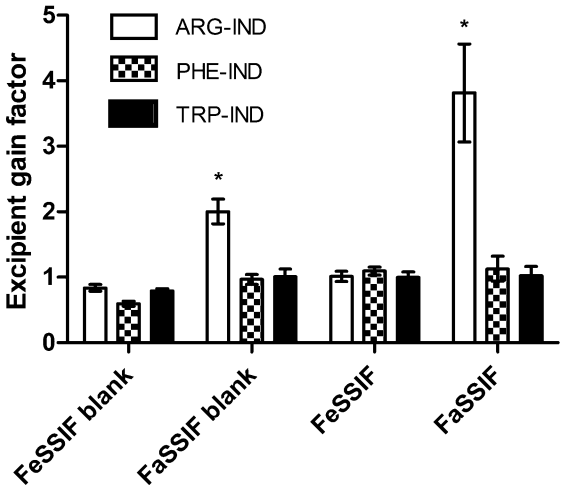

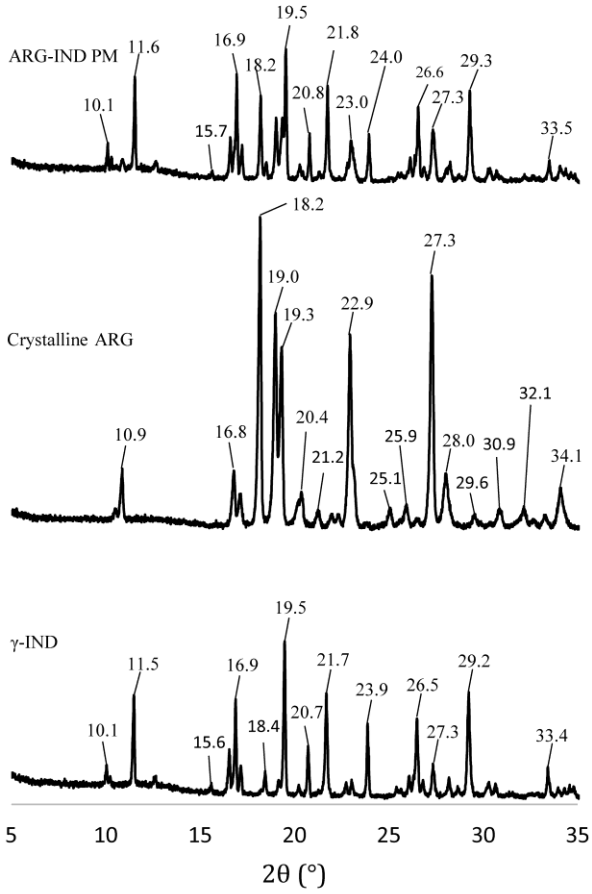
ARG-IND PM
10.1
11.6
15.7
16.9
18.2
19.5
20.8
21.8
23.0
24.0
26.6
27.3
29.3
33.5
Crystalline ARG
10.9
16.8
18.2
19.0
19.3
20.4
21.2
22.9
25.1
25.9
27.3
28.0
29.6
30.9
32.1
34.1
γ-IND
10.1
11.5
15.6
16.9
18.4
19.5
20.7
21.7
23.9
26.5
27.3
29.2
33.4
5
10
15
20
25
30
35
2θ (°)

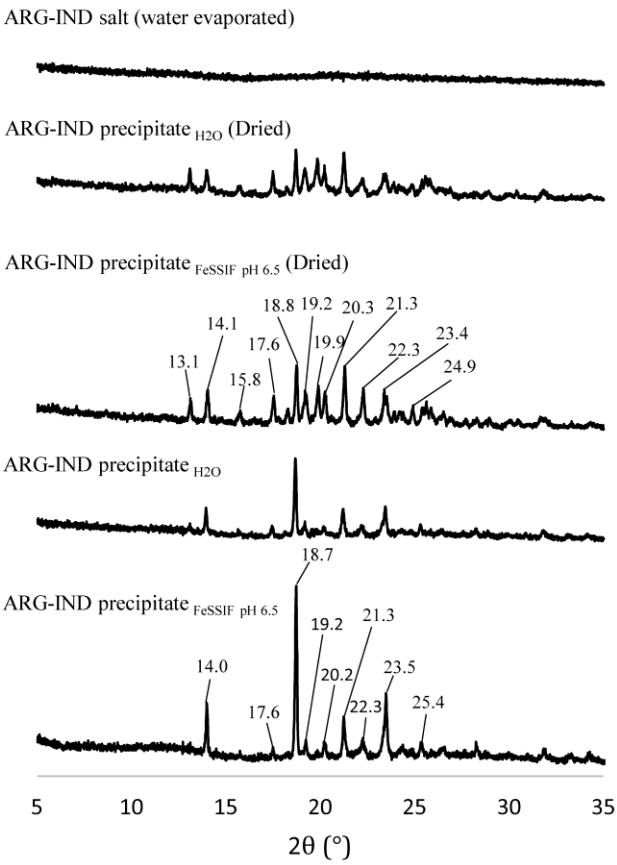
ARG-IND salt (water evaporated)
ARG-IND precipitate H2O (Dried)
ARG-IND precipitate FeSSIF pH 6.5 (Dried)
13.1
14.1
15.8
17.6
18.8
19.2
19.9
20.3
21.3
22.3
23.4
24.9
ARG-IND precipitate H2O
ARG-IND precipitate FeSSIF pH 6.5
14.0
17.6
18.7
19.2
20.2
21.3
22.3
23.5
25.4
5
10
15
20
25
30
35
2θ (°)

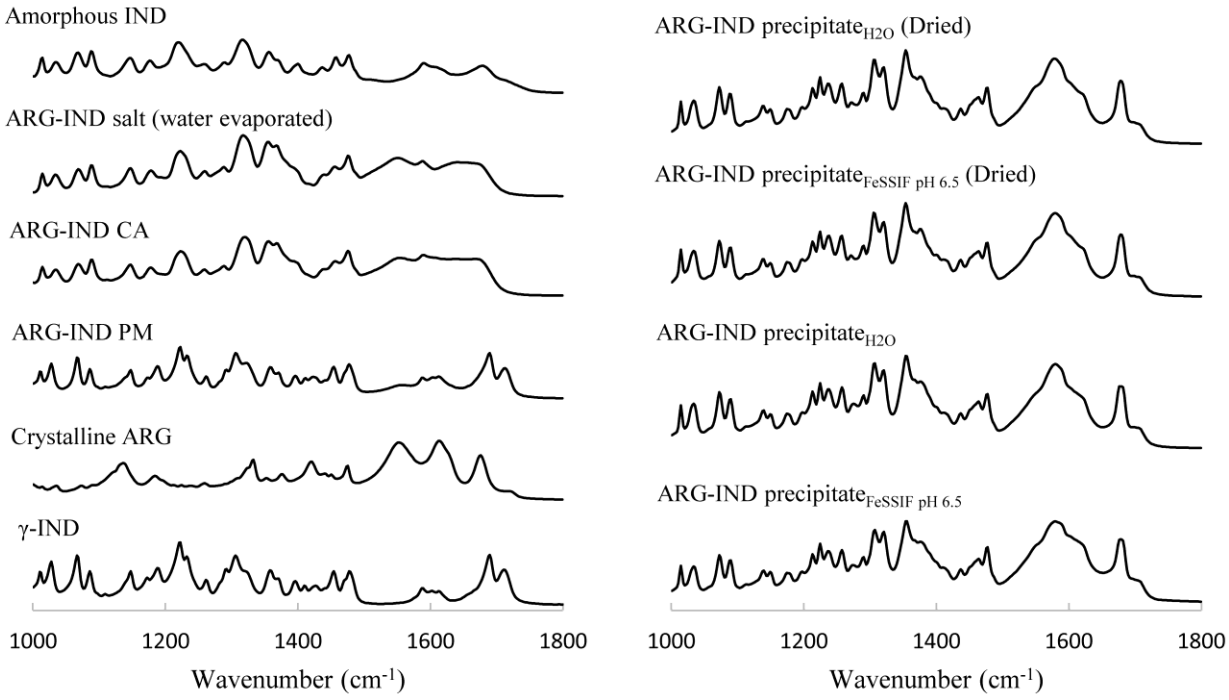

	$C_{72\ cryst}$	$C_{72\ amorph}$
FeSSIF blank	22 µg/ml	26 µg/ml
FaSSIF blank	480 µg/ml	480 µg/ml
FeSSIF	180 µg/ml	120 µg/ml
FaSSIF	620 µg/ml	830 µg/ml

Material	T_g (°C) (Measured)	T_g (°C) [24]
ARG-IND	62.9 ± 0.8	64.1 ± 1.4
PHE-IND	55.3 ± 0.4	47.8 ± 2.9
TRP-IND	62.7 ± 7.0	68.7 ± 2.6
IND	45.9 ± 0.1	36.7 ± 0.8

	$AUC_{0\text{-}72\ FeSSIF\ blank}$ (mg*h/ml)	$AUC_{0\text{-}72\ FaSSIF\ blank}$ (mg*h/ml)	$AUC_{0\text{-}72\ FeSSIF}$ (mg*h/ml)	$AUC_{0\text{-}72\ FaSSIF}$ (mg*h/ml)
ARG-IND	2.0 ± 0.2	97 ± 4.7*	17 ± 1.1*	150 ± 3.7*
PHE-IND	1.7 ± 0.2	36 ± 1.5	12 ± 0.6	41 ± 5.0
TRP-IND	1.7 ± 0.2	36 ± 3.1	12 ± 0.4	43 ± 5.4
IND	1.4 ± 0.2	33 ± 1.5	12 ± 0.1	43 ± 4.0

Dissolution/precipitation medium	SF_{DISSO}	SF_{PRECIP}
FaSSIF blank	1,13 ± 0,02	2,28 ± 0,20
FaSSIF	1,15 ± 0,18	1,10 ± 0,14
FeSSIF blank	1,13 ± 0,03	3,42 ± 0,18
FeSSIF	0,89 ± 0,05	3,80 ± 0,23

Graphical abstract